JPn Neuroscience

The Journal of Physiology

J Physiol 591.4 (2013) pp 955–972

Different NMDA receptor subtypes mediate induction of long-term potentiation and two forms of short-term potentiation at CA1 synapses in rat hippocampus *in vitro*

Arturas Volianskis[1,2,3], Neil Bannister[1,2], Valerie J. Collett[1,2], Mark W. Irvine[2], Daniel T. Monaghan[4], Stephen M. Fitzjohn[1], Morten S. Jensen[3], David E. Jane[2] and Graham L. Collingridge[1,2,5]

MRC Centre for Synaptic Plasticity, Departments of [1]Anatomy, and [2]Physiology & Pharmacology, University of Bristol, Bristol, UK
[3]Department of Anatomy, University of Aarhus, Aarhus, Denmark
[4]Department of Pharmacology and Experimental Neuroscience, University of Nebraska Medical Center, Omaha, USA
[5]Department of Brain and Cognitive Sciences, Seoul National University, Gwanak-gu, Seoul, Korea

Key points

- *N*-Methyl-D-aspartate receptor (NMDAR)-dependent potentiation of synaptic transmission is widely accepted as a cellular model of learning and memory.
- It is most often studied in the CA1 area of rat hippocampal slices where it comprises a decremental and a sustained phase, which are commonly referred to as short-term potentiation (STP) and long-term potentiation (LTP), respectively.
- In this study we show for the first time that STP and LTP are triggered by the activation of different classes of NMDARs and that STP itself comprises two pharmacologically and kinetically distinct components.
- We suggest that the mechanistic separation of STP and LTP is likely to have important functional implications in that these two forms of synaptic plasticity can subserve unique physiological functions in a behaving animal.

Abstract Potentiation at synapses between CA3 and the CA1 pyramidal neurons comprises both transient and sustained phases, commonly referred to as short-term potentiation (STP or transient LTP) and long-term potentiation (LTP), respectively. Here, we utilized four subtype-selective *N*-methyl-D-aspartate receptor (NMDAR) antagonists to investigate whether the induction of STP and LTP is dependent on the activation of different NMDAR subtypes. We find that the induction of LTP involves the activation of NMDARs containing both the GluN2A and the GluN2B subunits. Surprisingly, however, we find that STP can be separated into two components, the major form of which involves activation of NMDARs containing both GluN2B and GluN2D subunits. These data demonstrate that synaptic potentiation at CA1 synapses is more complex than is commonly thought, an observation that has major implications for understanding the role of NMDARs in cognition.

(Resubmitted 24 October 2012; accepted after revision 7 December 2012; first published online 10 December 2012)
Corresponding author A. Volianskis: MRC Centre for Synaptic Plasticity, School of Physiology & Pharmacology, Dorothy Hodgkin Building, Whitson Street, Bristol BS1 3NY, UK. Email: a.volianskis@bristol.ac.uk

Abbreviations: ANOVA, analysis of variance; AP5, D-2-amino-5-phosphonopentanoate; DT, Dunnett's Multiple Comparison Test; EPSCs, excitatory postsynaptic currents; f-EPSPs, field excitatory postsynaptic potentials; IC_{50}, half maximal inhibitory concentration; LTP, long-term potentiation; NKMCT, Newman–Keuls Multiple Comparison Test; NMDARs, *N*-methyl-D-aspartate receptors; SEM, standard error of the mean; STP, short-term potentiation; TBS, theta-burst stimulation.

A. Volianskis and N. Bannister contributed equally to this work.

DOI: 10.1113/jphysiol.2012.247296

Introduction

Long-term potentiation (LTP; Bliss & Lomo, 1973) at synapses between CA3 and CA1 pyramidal neurons is dependent on the synaptic activation of *N*-methyl-D-aspartate receptors (NMDARs) (Collingridge *et al.* 1983). It is readily induced in hippocampal slices by a brief high-frequency tetanus (Andersen *et al.* 1977) or by theta patterns of stimulation (Larson *et al.* 1986). The brief period(s) of high-frequency stimulation relieve the Mg^{2+} block from the NMDARs leading to an elevation of $[Ca^{2+}]_i$ and induction of potentiation (see Bliss & Collingridge, 1993). Two phases of NMDAR-dependent LTP induced by high-frequency stimulation have been described: (1) a transient phase, often referred to as short-term potentiation (STP) or sometimes as transient LTP (t-LTP), that declines to (2) a stable phase, referred to as early LTP (e-LTP), sustained LTP (s-LTP) or, most commonly, simply LTP.

Whether STP and LTP share a common induction mechanism (Gustafsson & Wigstrom, 1990; Hanse & Gustafsson, 1994) or not (Larson *et al.* 1986; Kauer *et al.* 1988; Schulz & Fitzgibbons, 1997; Volianskis & Jensen, 2003) remains unresolved. NMDARs are implicated in both processes as high concentrations of the highly selective NMDAR antagonist D-2-amino-5-phosphonopentanoate (AP5; Davies *et al.* 1981) block both the transient and the sustained phases of LTP (Larson & Lynch, 1988; Anwyl *et al.* 1989; Malenka, 1991; Schulz & Fitzgibbons, 1997; Volianskis & Jensen, 2003). However, it appears that STP and LTP have a different concentration dependency to AP5. A low concentration of AP5 is sufficient to block LTP (Malenka, 1991; Liu *et al.* 2004) whereas higher concentrations alone (Malenka, 1991) or in combinations with other NMDAR antagonists (Pananceau & Gustafsson, 1997) are needed to block STP. It has been assumed that this relates to the level of activation of NMDARs, with a strong activation required to enable potentiation to persist into the sustained phase (Gustafsson & Wigstrom, 1990; Hanse & Gustafsson, 1994).

NMDARs are tetra-heteromeric assemblies, most commonly made up of two GluN1 and two GluN2 subunits (GluN2A–D), named according to International Union of Basic and Clinical Pharmacology nomenclature (Collingridge *et al.* 2009). It has been suggested that different NMDAR subtypes may affect the direction of synaptic plasticity (Hrabetova *et al.* 2000; Liu *et al.* 2004; Massey *et al.* 2004), although no firm rule exists (Berberich *et al.* 2005, 2007; Weitlauf *et al.* 2005; Bartlett *et al.* 2007; Li *et al.* 2007). In the present study we explored, for the first time, the possibility that different subtypes of NMDARs are involved during induction of different temporal phases of synaptic plasticity by studying potentiation at CA1 synapses in the hippocampus. We find that NMDAR subtype involvement in the induction of STP and LTP is complex. LTP involves the activation of NMDARs that contain GluN2A and GluN2B subunits, expressed most probably as a combination of diheteromeric GluN1/GluN2A and triheteromeric GluN1/GluN2A/GluN2B assemblies. Surprisingly, STP comprises two pharmacologically distinct components. One component of STP, which we term STP_1, is induced through activation of NMDARs that contain the GluN2A subunit. STP_1 could not be pharmacologically isolated from LTP. Induction of the second component of STP, which we term STP_2, is mediated through activation of GluN2B- and GluN2D-containing NMDARs. STP_2 can be readily induced following complete pharmacological block of LTP and STP_1 and decays more slowly than STP_1. These data constitute the first evidence that different NMDAR subtypes mediate the induction of temporally distinct components of synaptic plasticity and that STP comprises two mechanistically distinct processes.

Methods

Slice preparation and electrophysiological recordings

Experiments were performed after institutional approval, according to the UK Scientific Procedures Act, 1986 and European Union guidelines for animal care. Animals were killed by an overdose of isoflurane anaesthesia and death was confirmed by a permanent cessation of the circulation (Schedule 1). As described previously (Volianskis & Jensen, 2003), transverse slices (400 μm) were cut from the septal end of the hippocampus (male Wistar rats, ≈300 g) using a McIllwain tissue chopper. Slices were pre-incubated for at least 2 h at room temperature before the start of the experiments. During the experiments, the slices were perfused with saline (in mM: 124 NaCl, 3.5 KCl, 1.25 NaH_2PO_4, 26 $NaHCO_3$, 2 $CaCl_2$, 2 $MgSO_4$ and 10 glucose, saturated with 95% O_2 – 5% CO_2 at 37 °C) and maintained submerged (32.5°C).

Field excitatory postsynaptic potentials (f-EPSPs) were recorded in the CA1-B area of stratum radiatum using glass electrodes filled with saline solution, amplified (AxoPatch 1D; Axon Instruments, Union City, CA, USA), filtered at 4 kHz (CyberAmp 380; Axon) and digitized (Digidata 1440A; Axon) at 100 kHz. The Schaffer collaterals were stimulated (stimulus duration 100 μs, Master 8; A.M.P.I., Jerusalem, Israel) via a bipolar concentric tungsten electrode (World Precision Instruments (WPI), Sarasota, FL, USA). Stimulation current (A385; WPI) was fixed to three times the threshold for evoking f-EPSPs. The signals were recorded using pCLAMP software (Axon). f-EPSPs were evoked at a baseline frequency of 0.067 Hz. Potentiation was induced by a theta-burst tetanization protocol (four stimuli at 100 Hz,

repeated 10 times at a frequency of 5 Hz). Following delivery of the tetanus, stimulation was paused for 3 min. To estimate the maximum amount of NMDAR-dependent potentiation (P_{MAX}) we used an average of the first four f-EPSPs following the 3 min pause in stimulation. In some experiments we paused stimulation for a further 30 min following recording of P_{MAX}. In experiments, which used NMDA antagonists, compounds were bath applied for 30 min before the induction of potentiation and then washed out following recording of P_{MAX}.

Whole-cell voltage clamp recordings were made from the cell bodies of identified (using differential interference contrast optics) pyramidal neurons in the CA1 region. Patch pipettes (3–5 MΩ) were filled with an internal solution containing (in mM) $CsMeSO_3$, 130; NaCl, 8; Mg-ATP, 4; Na-GTP, 0.3; EGTA, 0.5; Hepes 10; QX-314, 5; BAPTA, 10; which had an osmolarity of 280 mOsm and pH of 7.2. Only experiments where there was less than 20% change in R_s (series resistance) were included in analysis. Recordings were made with an Axon 700B amplifier and digitized at a sampling rate of 10 kHz, using a CED 1401 A/D board with Signal Version 2 software. Excitatory postsynaptic currents (EPSCs) were evoked by extracellular stimulation of Schaffer collaterals in stratum radiatum using a monopolar stimulating electrode at a rate of either 0.05 or 0.017 Hz. To isolate the NMDAR-mediated component of the EPSC, NBQX (2,3-dihydroxy-6-nitro-7-sulfamoylbenzo(*F*)quinoxaline, 5 μM) and picrotoxin (50 μM) were included in the bath solution and the cell was voltage clamped at –30 mV. The amplitude of NMDAR-mediated EPSCs was measured offline, from 1 min averages. EPSCs were fitted using a double exponential function.

Analyses of electrophysiological data

The rate of rise of f-EPSPs was measured before (baseline) and after the induction of potentiation and normalized to baseline (defined as 100%). The increase in synaptic transmission was expressed as the amplitude of potentiation by subtracting the control level (100%) from the normalized rising rates of f-EPSPs. This permits the amplitudes of transient and sustained phases of potentiation to be compared directly in terms of percentage increase over baseline. Results are presented by plots of mean estimates of potentiation amplitudes (± standard error of the mean, SEM) plotted over time.

The amplitudes of transient (STP) and sustained (LTP) phases of potentiation and the decay time constants of the transient phases (τ) were determined by a mono-exponential fitting routine ($P = \text{LTP} + \text{STP}\ e^{-t/\tau}$, Levenverg–Marquardt method) and by double exponential fits using Prism (GraphPad Software, Inc., La Jolla, CA, USA). Mean estimates of STP and LTP, which were derived from individual experiments, were used to generate the exponential decay functions that are shown overlaid upon the mean data sets to illustrate the goodness of the fits. Statistical comparisons of single and double exponential fits of averaged datasets (see Fig. 9) were done using Prism.

STP is characterized by both its amplitude (percentage increase over baseline) and its duration (τ). We have therefore defined the amount of STP expressed in an individual experiment in terms of the area under its exponential decay ($\text{STP} = \text{amplitude} \times \tau$) whereas the amount of LTP was defined simply as its amplitude (percentage increase over baseline). Effects of NMDAR antagonists on induction of STP and LTP were quantified in individual experiments in terms of percentage reduction (block) in the amount of STP and in the amplitude of LTP relative to their mean levels in control experiments (i.e. without the application of antagonists). These data were pooled for each concentration of an antagonist (mean ± SEM) and used to construct concentration–response curves describing the antagonist's effects on STP and LTP. The data were fit by single or biphasic sigmoidal concentration–response curves to assess the fitted curves statistically and to interpolate the half maximal inhibitory concentration (IC_{50}) values (Prism).

Analyses of NMDAR antagonists' effects on recombinant NMDARs expressed in HEK293 cells

The full-length cDNAs encoding rat NMDAR subunits GluN1a and GluN2B, kindly provided by S. Nakanishi (Institute for Immunology, Kyoto University, Japan), were subcloned into the mammalian expression vector pcDNA1/Amp (Invitrogen, Carlsbad, CA, USA). GluN2A in the RK7 vector was a generous gift from P. Seeburg (University of Heidelberg ZMBH, Heidelberg, Germany). Cell transfection was carried out as described previously (Collett & Collingridge, 2004; Bartlett *et al.* 2007). Briefly, HEK293 cells were maintained in culture at 37°C, plated on coverslips, then transiently transfected using SuperFect (Qiagen, Valencia, CA, USA) with a molar ratio of cDNA for GluN1a/GluN2 of 1:3, to give optimal expression of NMDARs (Chazot *et al.* 1994). After transfection, the cells were maintained for 24 h in a glutamine-free medium containing 100 μM D-AP5 to prevent activation of expressed receptors (Anegawa *et al.* 1995).

As described previously (Bartlett *et al.* 2007), transfected cells were washed and loaded with the calcium indicator Fluo3-AM (5 μM; Sigma, St Louis, MO, USA) in Hepes-buffered saline (HBS) and subsequently viewed on a confocal microscope (MRC 1024; Bio-Rad, Hercules, CA, USA) equipped with an argon laser. Cells were continuously perfused with HBS containing glycine (10 μM) at a rate of 3 ml min^{-1}. NMDA (with 10 μM

glycine) was applied in the presence or absence of the antagonists. An increase in fluorescence intensity, in response to NMDA, identified cells containing functional receptors. During an experiment NMDA (15 μM, 40 s) was applied at 15 min intervals: two responses in control buffer were obtained, followed by two in the presence of the antagonist and a further two in the control buffer. Acquired images were analysed using Scion Image (Scion Corporation, Frederick, MD, USA). For each recording the peak fluorescence (measured as pixel density) of each cell in response to NMDA was normalized to its pre-agonist level because of cell-to-cell variation in size, transfection level and indicator loading. Inhibition was determined by comparing the second application of NMDA in the presence of antagonist with the mean of the second control responses before and after antagonist. Data are presented as mean percentage inhibition (± SEM) *versus* antagonist concentration. IC_{50} values were calculated using non-linear regression analysis (Prism).

Chemicals

D-AP5 was acquired from Ascent (Bristol, UK). Ro 25-6981 was obtained from Tocris (Bristol, UK). NVP-AAM077 was a generous gift from Novartis Pharma AG, Switzerland, and UBP145 was synthesized in house as described previously (Morley *et al.* 2005; Costa *et al.* 2009). NMDAR antagonists were prepared as stock solutions, stored frozen and added to perfusion saline as indicated in the Results. All other chemicals and salts were from Fisher Scientific (Loughborough, UK) or Sigma (Dorset, UK).

Statistical analyses

Analyses, statistical evaluation and presentation of the data were performed with Platin (custom build software, M.S.J.) and Prism IV (GraphPad Software, Inc.). Student's (two-tailed) *t* tests were used for either within- (paired) or between- (unpaired) group comparisons. One-way analysis of variance (ANOVA) followed by Dunnett's Multiple Comparison Test (DT) or Newman–Keuls Multiple Comparison Test (NKMCT) was used in cases of multiple comparisons. An *F* test was used for statistical evaluation of exponential and sigmoidal fits and for statistical comparison of IC_{50} values (Prism). Statistical differences were set at $P < 0.05$.

Results

Differential effects of AP5 on STP and LTP

In control experiments (Fig. 1*A*), f-EPSPs were potentiated by theta-burst stimulation (TBS). The initial potentiation (P_{MAX}), which was measured at 4 min post-tetanus to avoid contamination from post-tetanic potentiation, was 117 ± 7% (increase over baseline, $n = 25$). STP declined with a mean time constant of 16.0 ± 1.4 min to a stable LTP of 50 ± 5% (increase over baseline, Fig. 1*A*). The amplitude of STP, calculated from an exponential fit to the data, was 61 ± 4%, and so was roughly equivalent in magnitude to the LTP that followed. Similar values for STP and LTP were obtained in experiments in which a 30 min pause in stimulation was imposed following TBS (P_{MAX} 111 ± 8%, STP 54 ± 6%, tau 16.1 ± 2.5 min, LTP 48 ± 7%, $n = 14$, Fig. 1*A*), confirming the findings of previous studies showing that STP can be stored after a pause in stimulation (Volianskis & Jensen, 2003; Volianskis *et al.* 2010).

To investigate the NMDAR dependence of STP and LTP, AP5 was applied during baseline and TBS. AP5 (30–100 μM) blocked the induction of both STP and LTP (Fig. 1*A*). At lower concentrations, however, AP5 had strikingly different effects on STP and LTP (Fig. 1*B*). Similar differential effects of AP5 were observed in experiments with and without a pause in stimulation and so the data from both types of experiments were pooled (Fig. 1*C*). Notably, 0.3 μM AP5 reduced STP ($P < 0.01$, when compared to control, ANOVA, DT) without appreciably affecting LTP whilst 3 μM AP5 essentially blocked LTP ($P < 0.001$, when compared to control, DT), without further affecting STP to any significant extent (Fig. 1*C*). Construction of full concentration–response curves revealed that inhibition of LTP by AP5 was fit well with a single sigmoidal function (Fig. 1*D*, $IC_{50} \sim 1$ μM) whereas inhibition of STP was best fit with a double sigmoidal function with IC_{50} values that differed 65-fold (Fig. 1*D*). The differential sensitivity of the components of potentiation to AP5 is highly suggestive that more than one NMDAR subtype is activated during TBS and is responsible for LTP and the two components of STP.

Effects of antagonists on NMDAR subunits expressed in HEK293 cells

GluN2A, 2B and 2D NMDAR subtypes are expressed in the adult hippocampus (Thompson *et al.* 2002). To investigate their role in the induction of LTP we selected three additional subtype-selective antagonists: NVP-AAM077 (NVP; Auberson *et al.* 2002), Ro 25-6981 (Ro; Fischer *et al.* 1997) and UBP145 (UBP; Costa *et al.* 2009). The potency of these antagonists was assessed on NMDAR-mediated signals in HEK293 cells expressing recombinant rat GluN2A-, GluN2B- or GluN2D-containing receptors (Fig. 2). NVP showed a greater than 10-fold selectivity for GluN2A over GluN2B, separating the two subunits effectively at a concentration of 100 nM (Fig. 2*A*). It was also an effective inhibitor of GluN2D. Ro was highly potent at GluN2B but had no effect on either GluN2A

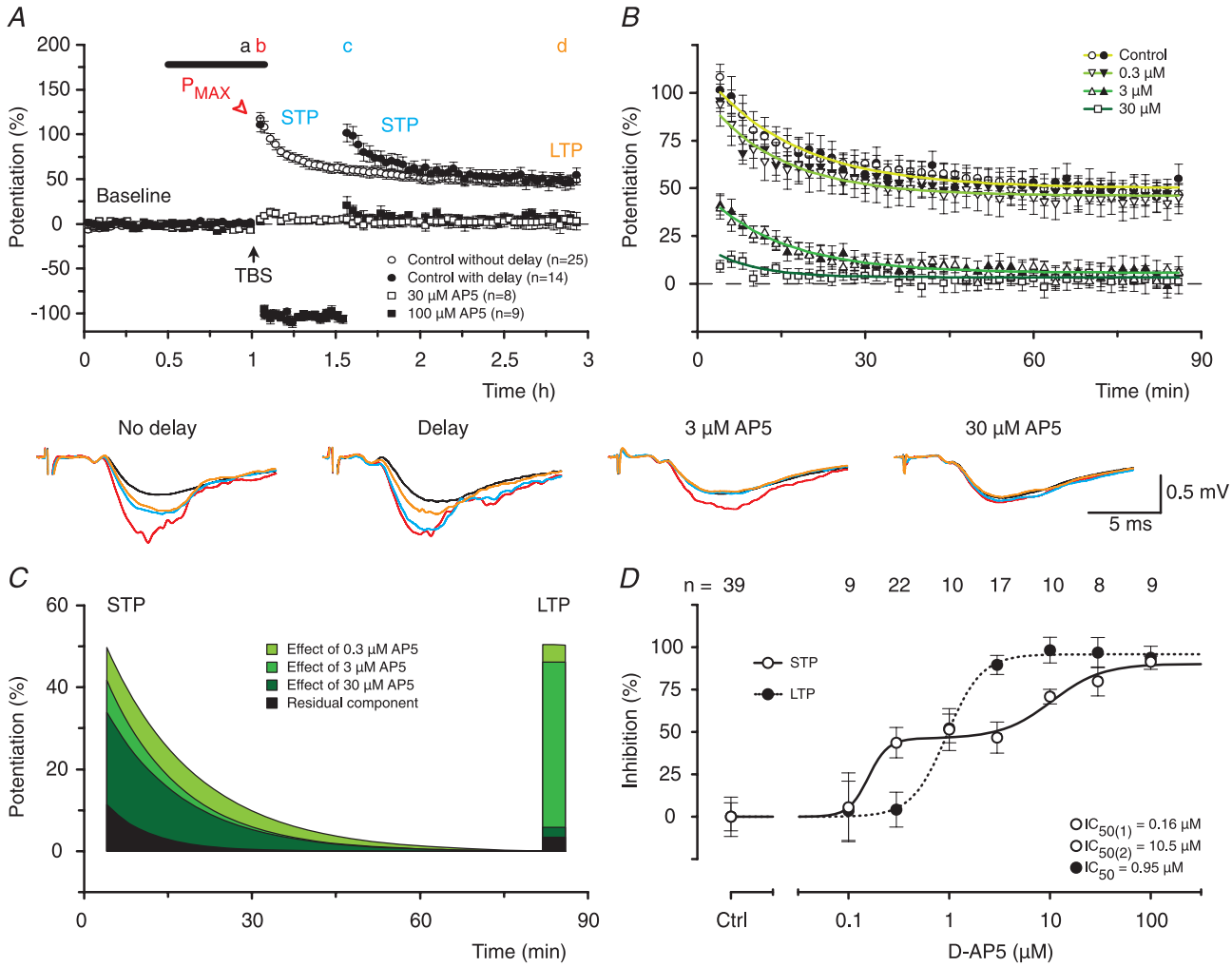

Figure 1. Complex inhibition of STP and LTP by AP5
A, mean time course of f-EPSP potentiation (open circles, ± SEM) showing that STP, which was induced by theta-burst stimulation (TBS, arrow), declines to a level of sustained LTP. When post-tetanic stimulation is delayed for 30 min STP does not decline significantly until the stimulation is resumed (filled circles). Both STP and LTP are blocked by high concentrations of the NMDAR antagonist D-AP5 (filled and open squares, with and without the delay in stimulation, respectively). The thick line indicates the time of application of AP5 and experiment numbers for each of the groups are indicated in the inset. Representative f-EPSPs before (black) and 4 min (red), 34 min (blue) and 120 min (orange) following TBS from experiments with and without a delay in test stimulation, and from experiments with AP5 are shown below the panel. Timing is indicated in the top of *A* by letters (a–d), which correspond in colour to the f-EPSPs. Calibration bar is shown in the inset. *B*, declining phases of potentiation are shown for experiments without the delay in stimulation (open symbols) and for experiments with the delay in stimulation (filled symbols). In this and subsequent figures, there are no differences between experiments with and without the delay and the combined data sets can be described by single exponential functions (overlaid coloured lines). The darkness of the green lines corresponds to the concentration of AP5. *C*, exponential phases from *B* for different concentrations of AP5 (inset) are shown after subtraction of LTP; the data from experiments with and without the delay in stimulation have been combined. The area under the curves reflects the amount of STP. LTP levels for each of the conditions are visualized as bars. Note that 0.3 μM AP5 substantially reduced STP but had little effect on LTP (light green) whereas 3 μM AP5 blocked LTP without having much of an additional effect on STP (mid green). *D*, concentration–response curves for inhibition of STP and LTP by AP5. The inhibition of STP by AP5 was best described by a double sigmoidal curve (continuous line) with ~65-fold difference between the low (0.16 μM) and the high (10.5 μM) IC_{50} values. A single sigmoidal curve (dotted line, IC_{50} = 0.95 μM) was sufficient to describe the block of LTP. Each point is the mean ± SEM of values obtained from between 8 and 39 separate slices. In this and subsequent concentration–response curves, the numbers of experiments per group are shown above the graph.

or GluN2D up to concentrations of around 10 μM, above which it inhibited GluN2A but not GluN2D (Fig. 2*B*). Notably, maximal inhibition of GluN2B by Ro depended on the agonist concentration (Fischer *et al.* 1997) whereas this was not the case for GluN2A. In contrast, UBP was approximately 10-fold more selective for GluN2D over either GluN2A or GluN2B (Fig. 2*C*). In conclusion, whilst no compound is ideal, the selectivity spectrum of these antagonists is sufficient to address the role of NMDAR subtypes in the induction of STP and LTP, provided that they are used in a comparative and quantitative manner.

Effects of antagonists on NMDAR-mediated EPSCs

Available data suggest that the pharmacology of recombinant NMDARs and native NMDARs is very similar (Buller *et al.* 1994; Christie *et al.* 2000; Feng *et al.* 2004). To establish the extent to which NMDARs containing GluN2A, 2B and 2D subunits contributed to synaptically activated NMDARs in adult hippocampal slices we studied pharmacologically isolated NMDAR-EPSCs (Fig. 3). The high sensitivity of pharmacologically isolated NMDAR-EPSCs to both AP5 and NVP (IC_{50} of 0.6 and 0.03 μM, respectively) suggests that they are predominately mediated by an NMDAR containing the GluN2A subunit (Fig. 3*A* and *B*). Ro, however, had interesting effects. It inhibited NMDAR-EPSCs at concentrations much higher than those that blocked GluN1/GluN2B receptors, but much lower than those that blocked GluN1/GluN2A receptors in HEK293 cells (Fig. 3*C*). This intermediate sensitivity can most readily be explained by its actions on a GluN1/GluN2A/GluN2B triheteromer (see Hatton & Paoletti, 2005; Gray *et al.* 2011; Rauner & Kohr, 2011). In support of this, a related GluN2B selective antagonist ifenprodil has been shown to block around 20% of GluN1/GluN2A/GluN2B triheteromeric receptors at a concentration of 30 μM while being around 10 times less potent than Ro (Hatton & Paoletti, 2005). The low sensitivity of the NMDAR-EPSCs to inhibition by UBP demonstrates that GluN2D-containing receptors are unlikely to contribute to synaptic transmission (Fig. 3*D*). The sensitivity of the NMDAR-EPSC to higher

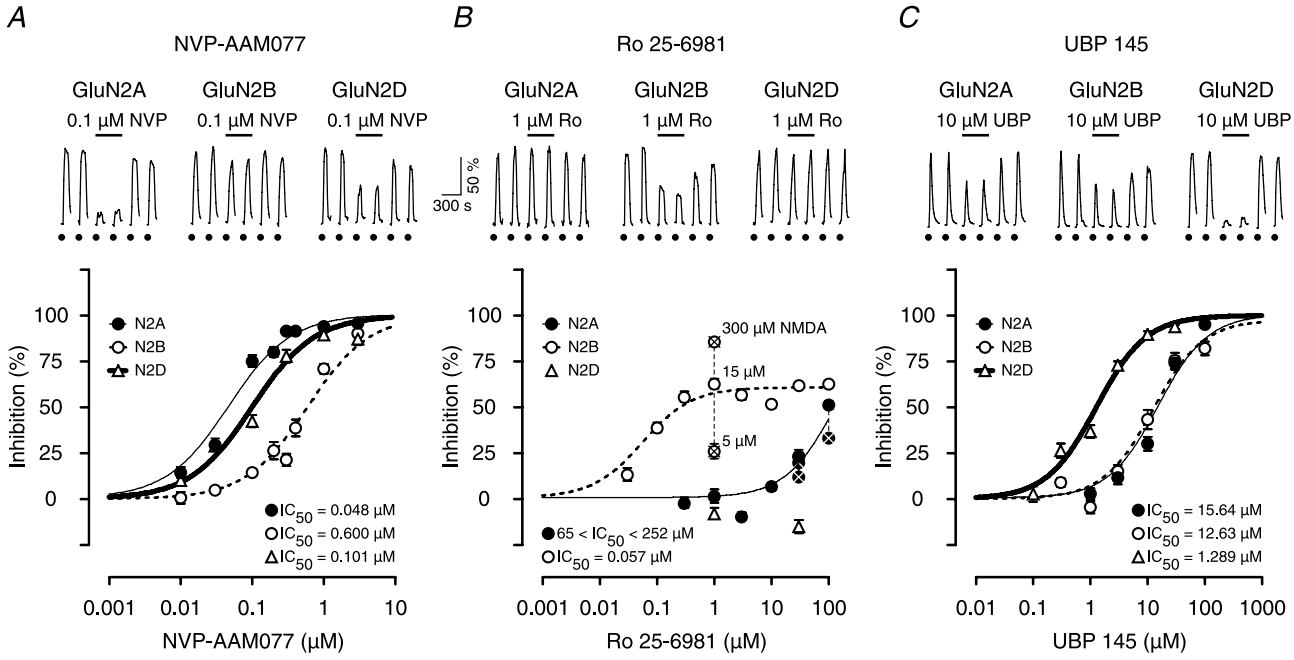

Figure 2. Effects of NVP, Ro and UBP on NMDA-evoked calcium signals in HEK293 cells
A, examples of calcium signals from single HEK293 cells transfected with GluN1a together with GluN2A, GluN2B or GluN2D receptors in response to 15 μM NMDA and 10 μM glycine (filled circles). Inhibition curves show that NVP is 13 times more potent at GluN2A (filled circles, thin line) than at GluN2B (open circles, dotted line) subunits but is only about two times more potent at Glu2NA *versus* GluN2D (open triangles, thick line). *B*, Ro is highly selective for GluN2B responses over a 1000-fold concentration range (open circles, dotted line). However, it inhibits GluN2A responses (filled circles, light line) at higher concentrations (i.e. > 10 μM). It did not antagonize GluN2D responses at the two concentrations tested (1 and 30 μM, open triangles). Note that the maximal inhibition of GluN2B (Fischer *et al.* 1997) but not GluN2A responses by Ro was agonist concentration-dependent (crossed open and closed symbols, respectively). *C*, UBP selectively inhibits GluN2D responses. Inhibition curves show that UBP is approximately 10-fold more potent on GluN2D (open triangles, thick line) than on GluN2A (filled circles, light line) or GluN2B (open circles, dotted line) receptors.

concentrations of UBP correlated closely with its actions on both GluN2A and 2B subunits.

Further support for the suggestion that the NMDARs, which mediate the EPSC, are composed of both GluN2A and 2B but not GluN2D subunits comes from analyses of EPSC decay. The decay of NMDAR-EPSCs recorded during baseline conditions could be described by a double exponential fit ($\tau_{Fast} = 56 \pm 1.3$ ms and

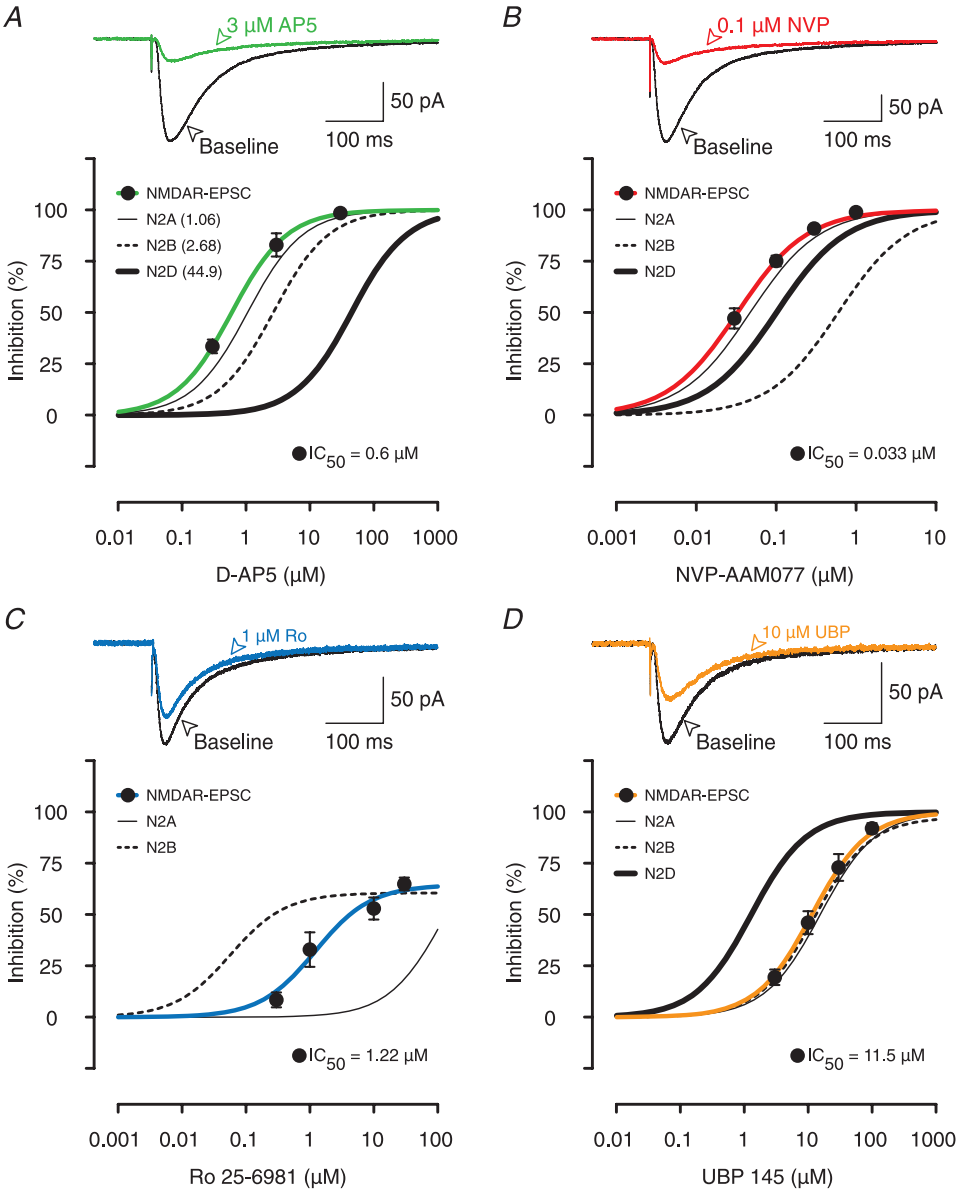

Figure 3. Effects of AP5, NVP, Ro and UBP on NMDAR-EPSCs
A, example traces show that 3 μM AP5 (green line) was able to block most of the NMDAR-EPSC (black line). Inhibition curves show that AP5 antagonized NMDAR-EPSCs (filled circles, green line) similarly to inhibition of GluN2A. Inhibition curves for GluN2A (thin black line), 2B (thin dotted line) and 2D (thick black line) subunits are re-plotted from data presented in Buller & Monaghan (1997); the IC_{50} values are given in parentheses. *B*, example traces show that 0.1 μM NVP was similar in its potency to 3 μM AP5 (*A*) in blocking NMDAR-EPSCs. NVP inhibited NMDAR-EPSCs (filled circles, red line) in parallel with inhibition of GluN2A subunits in HEK293 cells (thin black line). In *B–D*, the inhibition curves for recombinant receptors are re-plotted from Fig. 2. *C*, example traces show that 1 μM Ro (blue EPSC), which provided maximal inhibition of GluN2B-mediated responses in HEK293 cells (dotted inhibition curve), was not very effective in blocking the NMDAR-EPSC. Ro's inhibition of NMDAR-EPSCs (blue inhibition curve) fell in between its effects on GluN2A (thin black inhibition curve) and GluN2B subunits (dotted curve). *D*, UBP (filled circles, thick orange line) blocked NMDAR-EPSCs in a manner that was consistent with its effects on GluN2A and 2B subunits rather than GluN2D subunits. In each experiment, the data are mean ± SEM for between 4 and 7 neurons.

$\tau_{Slow} = 316 \pm 10$ ms), with about 80% of the total EPSC amplitude contributed by the fast component (Fig. 4*Aa–Ca*). This is considerably faster that the decay of GluN2D-containing receptors ($\tau_w > 1$ s), but is consistent with a response that involves both GluN2A and GluN2B subunits (Monyer *et al.* 1994; Vicini *et al.* 1998). NVP inhibited the fast component to a greater extent than the slow component of the NMDAR-EPSC, whereas Ro had the inverse effect. To visualize this differential sensitivity we scaled the amplitude of the slow component for each antagonist to the baseline response. As shown in Fig. 4*A* for 0.1 μM NVP, this led to a substantially smaller peak current, reflecting the greater sensitivity of the fast component to this antagonist. In contrast, Ro had a disproportionally smaller effect on the fast component, such that the scaled peak response was slightly larger (Fig. 4*B*). In contrast, UBP did not differentially affect the two components to any significant extent (Fig. 4*C*).

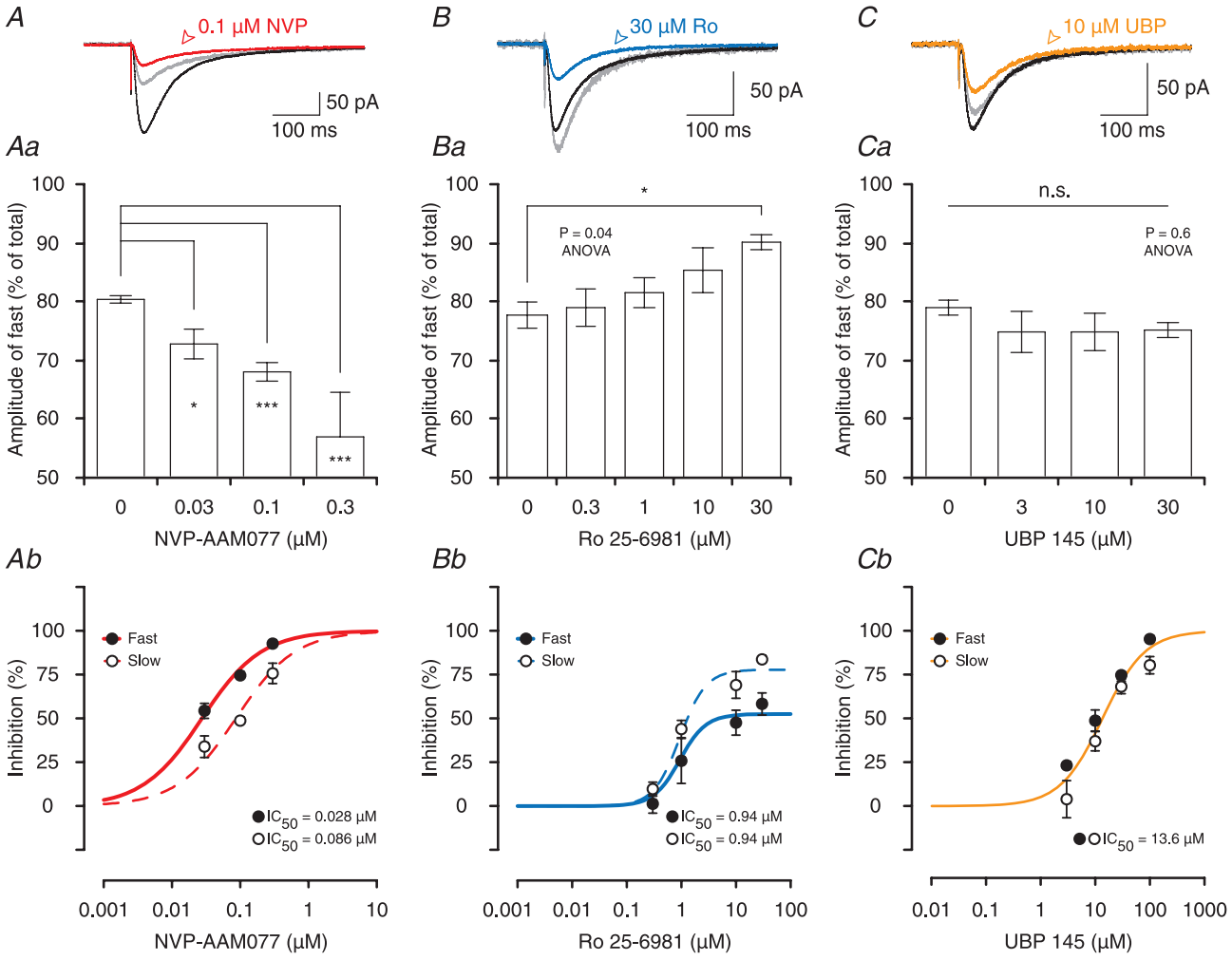

Figure 4. Effects of antagonists on kinetics of NMDAR-mediated EPSCs
A–C, effects of 0.1 μM NVP (red, *A*), 30 μM Ro (blue, *B*) and 10 μM UBP (orange, *C*) on NMDAR-EPSCs. The differential effects on the decays are visualized by scaling the slow component of the EPSCs (grey traces in each of the panels). This shows that NVP preferentially inhibits the amplitude of the fast component (EPSC does not scale back to its peak) whereas Ro is more effective in inhibiting the amplitude of the slow component (EPSC scales larger than its peak). UBP affected both components similarly. *Aa–Ca*, contribution of the fast component to the total EPSC amplitude decreases in experiments with NVP (*Aa*) and increases in experiments with Ro (*Bb*). Stars indicate significant differences between individual groups when compared to baseline ('0' concentration of an antagonist, DT). *Ca*, contribution of the fast component to the total EPSC does not change in experiments with UBP. *Ab–Cb*, concentration–response curves depicting the effects of NVP, Ro and UBP on the amplitudes of the fast and the slow components of NMDAR-EPSCs. *Ab*, NVP inhibits the fast component of the EPSC more potently than the slow ($P = 0.01$, *F* test). *Bb*, Ro is more efficacious in inhibiting the amplitude of the slow component than the fast but antagonizes both components with statistically indistinguishable IC_{50} values ($P = 0.8$). *Cb*, a single sigmoidal curve can describe the effect of UBP on both the fast and the slow component of NMDAR-EPSCs ($P = 0.1$).

To compare the effects of the three antagonists on the the fast and the slow components of the EPSC more precisely, their percentage inhibition was calculated from the two-exponential fits for each concentration of NVP (Fig. 4*Ab*), Ro (Fig. 4*Bb*) and UBP (Fig. 4*Cb*). With respect to Ro, both the fast and the slow components had identical sensitivity, in terms of IC_{50} values. This strongly suggests that a single population of GluN2B-containing NMDARs (most likely a triheteromeric receptor containing both GluN2A and GluN2B subunits) mediates the majority of the slow component and a significant fraction of the fast component. NVP was slightly more potent on the fast compared to the slow component, suggesting that its actions were mediated via two different receptor populations (most likely GluN2A-containing diheteromers and GluN2A- and GluN2B-containing triheteromers, respectively). UBP did not differentiate between the two components, consistent with a similar sensitivity on both GluN2A- and GluN2B-containing receptors.

In conclusion, these observations support a role of GluN2A- and GluN2B- but not GluN2D-containing NMDARs in the mediation of the EPSC and suggest that the involvement of GluN2B is as part of a triheteromeric assembly.

NVP preferentially inhibits LTP

In experiments in which GluN2A-containing receptors were antagonized by 30 nM NVP, LTP was reduced significantly ($P < 0.05$, DT) while STP was unaffected. LTP was eliminated but substantial STP remained in experiments with 100 nM NVP (Fig. 5*A*). This result was strikingly similar to experiments using 3 μM AP5,

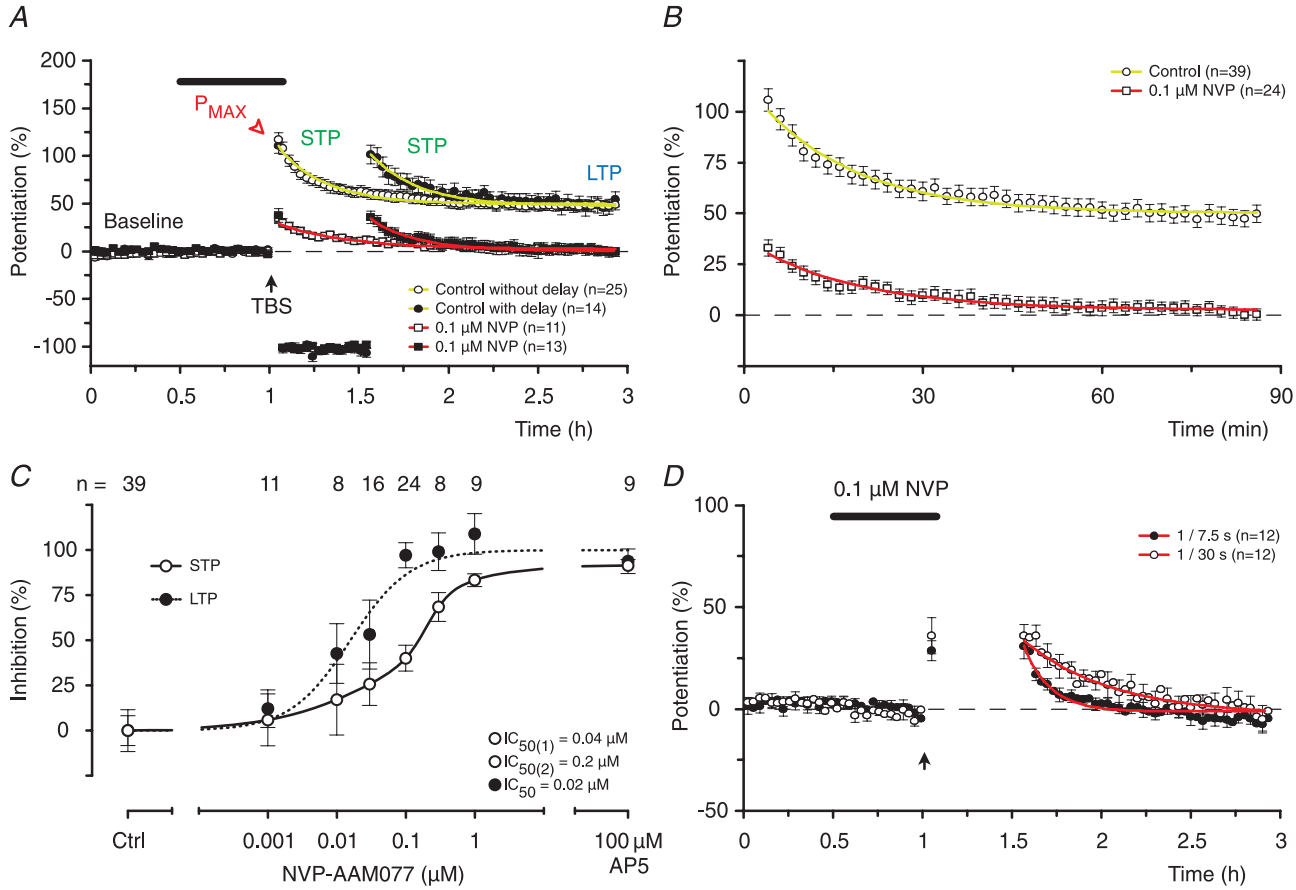

Figure 5. NVP is more potent at blocking LTP than STP
A, 0.1 μM NVP blocked LTP but spared a substantial amount of STP. There were no differences between experiments with (closed symbols) and without (open symbols) the delay in stimulation. *B*, pooled data from experiments with and without the delay in stimulation to illustrate STP in the absence of LTP. *C*, inhibition curves show that NVP was 2–10 times more potent at blocking LTP (filled circles) than STP (open circles), which was best fit by a double sigmoidal function. *D*, decay of pharmacologically isolated STP, recorded in the presence of 0.1 μM NVP, depends on stimulation. STP declined faster when the frequency of stimulation was increased ($\tau = 8.6 \pm 1.3$ min at 0.133 Hz, filled circles) and slower when the frequency of stimulation was decreased ($\tau = 30.0 \pm 3.4$ min at 0.033 Hz, open circles) when compared to the baseline frequency ($\tau = 19.5 \pm 1.9$ min at 0.067 Hz; $P < 0.05$ both cases, one-way ANOVA, NKMCT).

and again was independent of whether there was a pause in stimulation following TBS (Fig. 5*A* and *B*). Concentration–response curves, illustrated in Fig. 5*C*, show that a single sigmoidal function describes the inhibition of LTP ($IC_{50} = 0.02\ \mu M$) whereas STP is fitted preferentially with a bi-sigmoidal function ($IC_{50} = 0.04$ and $0.2\ \mu M$). The ability to preserve a substantial amount of STP following complete block of LTP (using 100 nM NVP) enabled us to investigate some of its properties in isolation. We observed that the rate of decay of this residual STP was related to the frequency of stimulation (Fig. 5*D*), as originally described for STP recorded in the presence of LTP and without a delay in stimulation (Volianskis & Jensen, 2003).

In summary, these results clearly demonstrate a role for GluN2A in the induction of LTP and one component of STP. The lack of complete inhibition of STP by GluN2A selective concentrations of NVP supports the conclusions drawn from the experiments using AP5 that STP comprises two pharmacologically distinct components.

Ro preferentially inhibits STP

Inhibition of GluN2B-containing NMDARs during induction of STP and LTP had dramatically different effects from inhibition of GluN2A-containing NMDARs (Fig. 6). For example, in experiments in which GluN2B-containing receptors were blocked with 1 μM Ro, the induction of STP was substantially reduced ($P < 0.001$, DT) but LTP was not inhibited significantly when compared to the control (Fig. 6*A* and *B*). A significant reduction of LTP was first detected when the concentration of Ro was increased to 5 μM (Fig. 6*C*), although no further

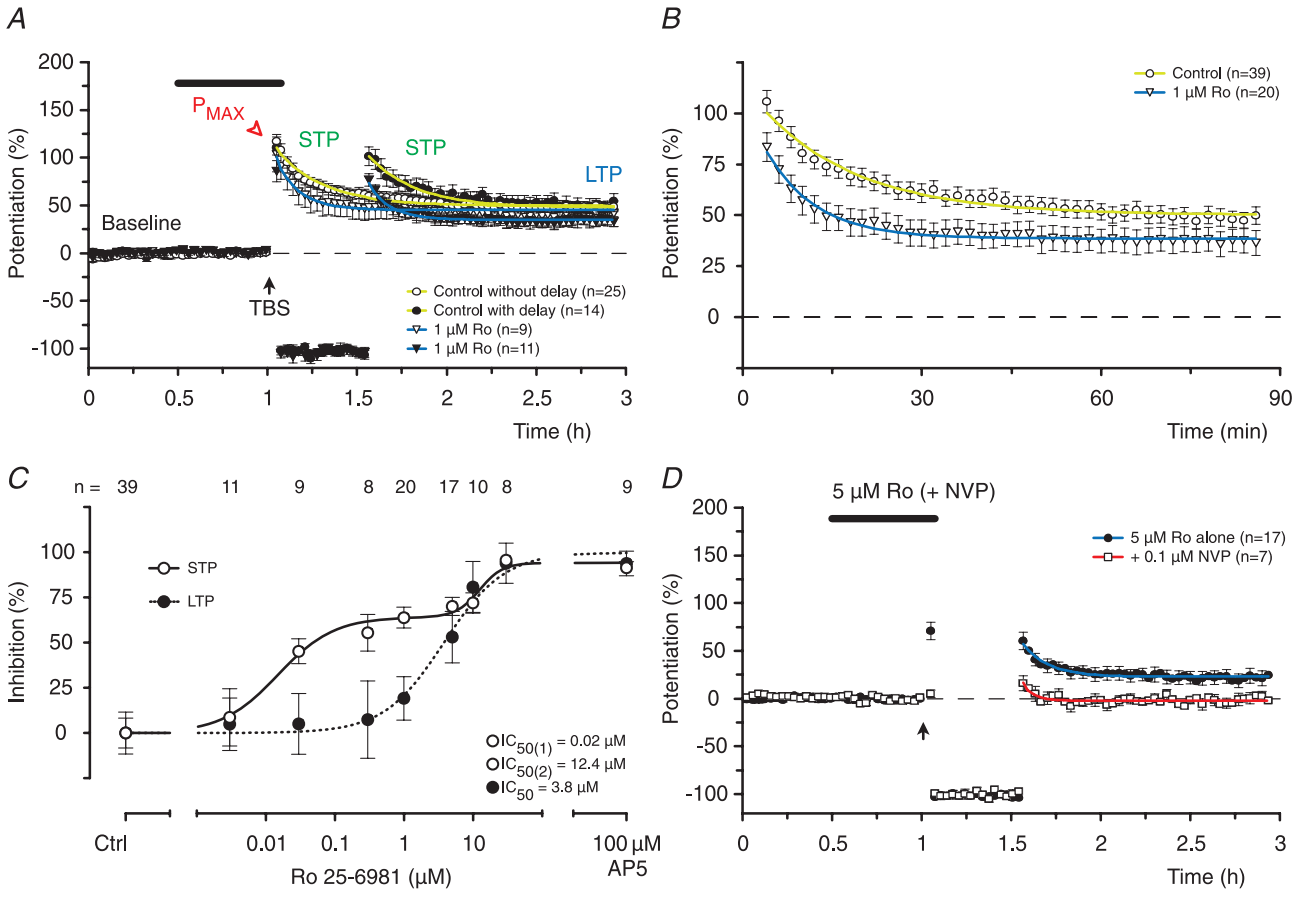

Figure 6. Ro is more potent at blocking STP than LTP
A, Ro (1 μM) reduced STP significantly ($P < 0.001$, ANOVA, DT) but had no effect on LTP ($P > 0.05$, ANOVA, DT). There were no differences between experiments with (closed symbols) and without (open symbols) the delay in stimulation. *B*, pooled data from experiments using 1 μM Ro with and without the delay in stimulation. *C*, Ro inhibited STP in a biphasic fashion (600-fold difference between the IC_{50} values) whereas a single sigmoidal curve was sufficient to describe its effects on LTP. Significant inhibition of LTP (when compared to the control) was seen with concentrations of Ro of 5 μM or more ($P < 0.01$, ANOVA, DT). *D*, the residual component of STP and LTP, recorded in the presence of a concentration of Ro (5 μM) that fully blocks one component of STP, is highly sensitive to 0.1 μM NVP (STP: $P < 0.05$, *t* test; LTP: $P < 0.05$, *t* test, when compared to 5 μM Ro alone).

inhibition of STP was observed at this concentration. However, higher concentrations of Ro blocked both LTP and the remaining component of STP. The inhibition of STP by Ro was fit by a double sigmoidal function, with IC_{50} values that differed around 600-fold (Fig. 6*C*). Such bi-modal inhibition further supports the notion that more than one NMDAR subtype is involved in the induction of STP. In contrast, a single sigmoidal function was again sufficient to describe the inhibition of LTP, with an IC_{50} value of 3.8 μM (Fig. 6*C*). This finding that STP is more sensitive than LTP to inhibition of GluN2B subunits by Ro further demonstrates the differential role of GluN2 subunits in these two phases of potentiation. The sensitivity of LTP to Ro, which parallels inhibition of the NMDAR-EPSC, is consistent with the involvement of triheteromeric NMDARs containing both the GluN2A and the GluN2B subunits in its induction (Hatton & Paoletti, 2005; Gray *et al.* 2011; Rauner & Kohr, 2011).

The ability of very low concentrations of Ro to antagonize one component of STP strongly suggests that NMDARs containing GluN2B subunits mediate induction of this component. The requirement for high concentrations of Ro to block the second component of STP could be due to its action at triheteromeric receptors containing both the GluN2A and the GluN2B subunits (i.e. similar to that observed with LTP). These findings, when taken together with the results using NVP, suggest that there exist two components of STP, which are induced differentially via the activation of NMDARs that are highly sensitive to antagonism of GluN2A or GluN2B subunits, respectively. In support of this notion, co-application of a GluN2A selective concentration of NVP (100 nM) with 5 μM Ro blocked the induction of STP (Fig. 6*D*).

UBP also preferentially inhibits STP

The effects of the GluN2D selective antagonist UBP were broadly similar to those of Ro (Fig. 7). For example, the induction of STP was substantially inhibited by 10 μM UBP whereas LTP was unaffected (Fig. 7*A* and *B*). LTP was first affected when the concentration of UBP was increased to 30 μM and all phases of potentiation were blocked at 100 μM (Fig. 7*C*). As with the other antagonists, the inhibition of LTP was best fit with a single sigmoidal function ($IC_{50} = 30$ μM) and STP with a double sigmoidal function (Fig. 7*C*).

The ability of the lower concentrations of UBP to inhibit one component of STP ($IC_{50} \sim 2$ μM) correlates with its ability to inhibit GluN2D subunits (Fig. 2*C*). The relatively insensitive component of STP was inhibited similarly to LTP (IC_{50} values for both ~ 30 μM) at concentrations at which UBP inhibits GluN2A and GluN2B subunits (Fig. 2*C*). This result is similar to that observed with Ro, and suggests that both Ro and UBP may be inhibiting the same component of STP. To test this directly, we applied a concentration of UBP (30 μM) that eliminated one component of STP and tested the sensitivity of the residual component to Ro. We selected a concentration of Ro (5 μM) that was also maximal for inhibition of the sensitive component to this antagonist. Addition of Ro had no further effect, demonstrating that the UBP- and Ro-sensitive components were identical. The residual component was, however, eliminated by a low concentration of AP5 (0.3 μM). These results provide strong evidence for the existence of two components of STP, one involving activation of GluN2A- and the other both GluN2B- and GluN2D-containing NMDARs.

Correlation between the inhibition of NMDAR-EPSCs and synaptic potentiation

The ability of the four NMDAR antagonists to inhibit NMDAR-EPSCs *versus* their ability to inhibit LTP and STP is illustrated in Fig. 8*A*–*C*. These plots show that antagonism of the NMDAR-EPSC strongly correlates with inhibition of LTP (Fig. 8*A*). Inhibition of one component of STP, which we now term STP_1, has the same rank order potency to the four antagonists as LTP (i.e. NVP > AP5 > Ro > UBP) and also correlates, although less strongly, with the inhibition of the NMDAR-EPSC (Fig. 8*B*). The second component of STP, termed STP_2, has a completely different rank order potency from STP_1 and LTP (Ro > NVP > UBP > AP5) and shows no correlation with the NMDAR-EPSC (Fig. 8*C*). Pharmacologically, therefore, STP_1 and STP_2 are distinct entities.

In addition to these different sensitivities to the antagonists, inhibition of these two components of STP was also qualitatively different. Inhibition of STP_1, using either 0.1 μM NVP or 3 μM AP5, resulted in a large reduction in the amplitude of STP with little effect on its decay time constant (Fig. 8*D* and *E*). Conversely, inhibition of STP_2 with either Ro (1 μM) or UBP (10 μM) resulted in a smaller effect on the amplitude of STP but dramatically increased its rate of decay (Fig. 8*F* and *G*). From this it can be concluded that these two components contribute differently to the expression of STP. For example, at a baseline stimulation rate of 0.067 Hz, the decay of the two components can be described with single exponentials of about 7 and 16 min, respectively. The relative size and kinetics of the three synaptic components (LTP, STP_1 and STP_2) are compared in Fig. 9.

Discussion

In the present study we have utilized four NMDAR antagonists to investigate the NMDAR subtypes involved in two temporally distinct forms of hippocampal synaptic plasticity, STP and LTP. We have found that inhibition

of LTP correlates closely with inhibition of the EPSC and involves activation of both GluN2A and GluN2B receptors, the latter most likely as part of a triheteromeric complex. In addition, we have found that STP comprises two pharmacologically and kinetically distinct components, the predominant one of which involves activation of GluN2B and GluN2D receptors.

Subtype selectivity of NMDAR antagonists

To investigate the role of NMDAR subtypes in LTP we have used four antagonists, the prototypic NMDAR antagonist AP5 and three antagonists showing a degree of selectivity towards the various subtypes. AP5, NVP and UBP are competitive antagonists, binding at the glutamate-binding site with a different potency at the different GluN2 subunits. The mechanism of action of the GluN2B-selective allosteric antagonist Ro is more complex in that it binds at the interface of the heterodimer, which is formed by GluN1 and GluN2B subunits (Karakas *et al.* 2011). The difference in the mechanisms of action of the antagonists can affect the interpretation of the results of the experiments, especially in the case of Ro, which is sensitive to a number of ambient factors modulating its potency. To be confident in the conclusions of our experiments we first characterized NVP, Ro and UBP in a recombinant receptor assay in HEK293 cells (Fig. 2) describing their selectivity. We then conducted the intracellular and extracellular studies in hippocampal slices and constructed full concentration–response curves for each of the conditions for each of the antagonists. In addition, we designed experiments in which antagonists with different mechanisms of action were co-applied to verify their synergistic effects and our conclusions.

We confirmed that NVP shows approximately 10-fold selectivity for GluN2A- *versus* GluN2B-containing receptors but found that GluN2D-containing receptors are also fairly sensitive to this antagonist (see

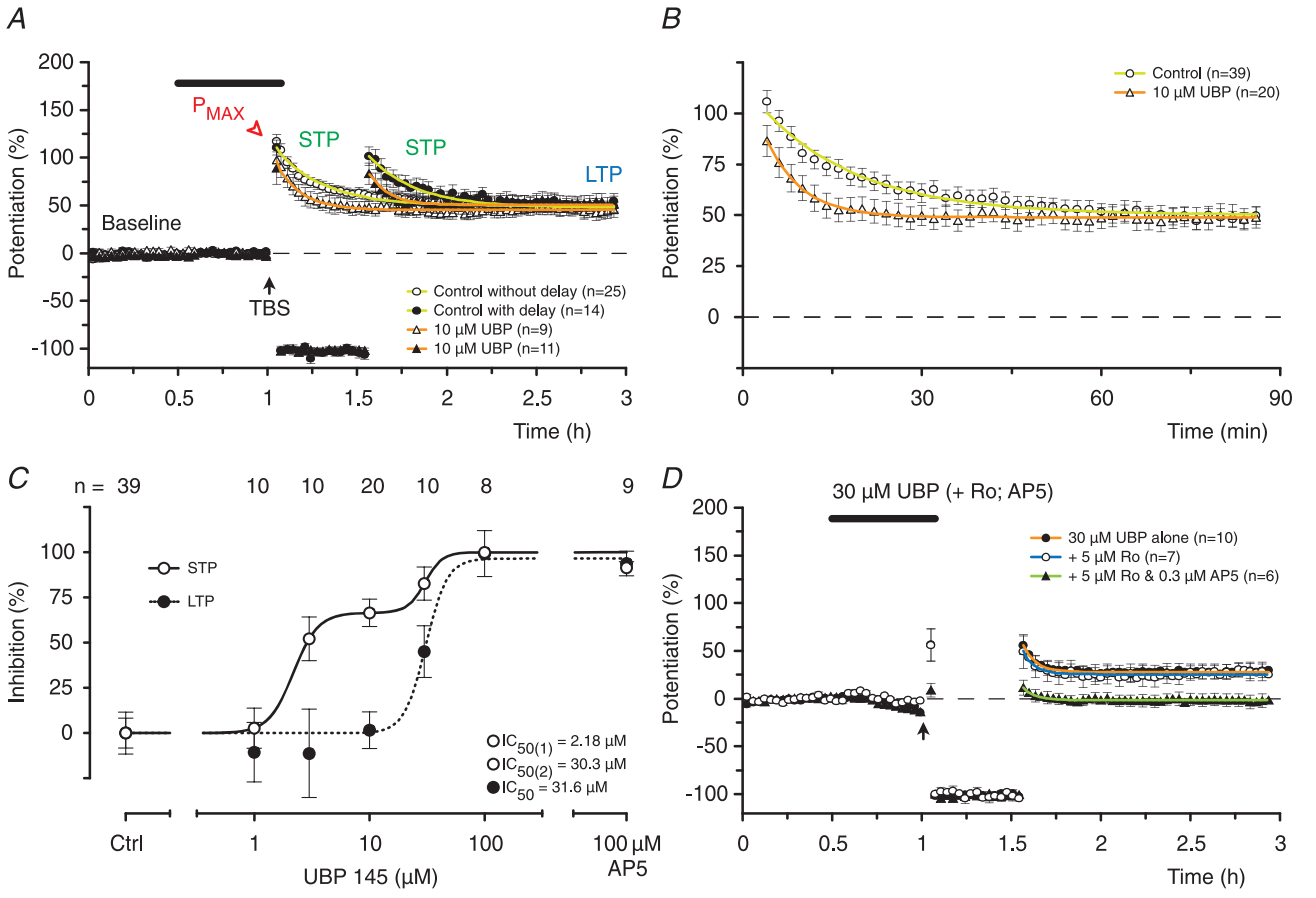

Figure 7. UBP is more potent at blocking STP than LTP
A, UBP (10 μM) reduced STP significantly ($P < 0.001$, ANOVA, DT) but had no effect on LTP ($P > 0.05$, ANOVA, DT). *B*, pooled data from experiments using 10 μM UBP, with and without the delay in stimulation. *C*, UBP inhibited STP in a biphasic fashion (14-fold difference between the IC_{50} values) whereas a single sigmoidal curve was sufficient to describe its effects on LTP. *D*, the residual components of STP and LTP, recorded in the presence of a concentration of UBP (30 μM) that fully blocks one component of STP, are unaffected by the addition of Ro (STP: $P = 0.6$, *t* test; LTP: $P = 0.7$, *t* test) but are eliminated by the further addition of 0.3 μM AP5 ($P < 0.05$, *t* test, both cases).

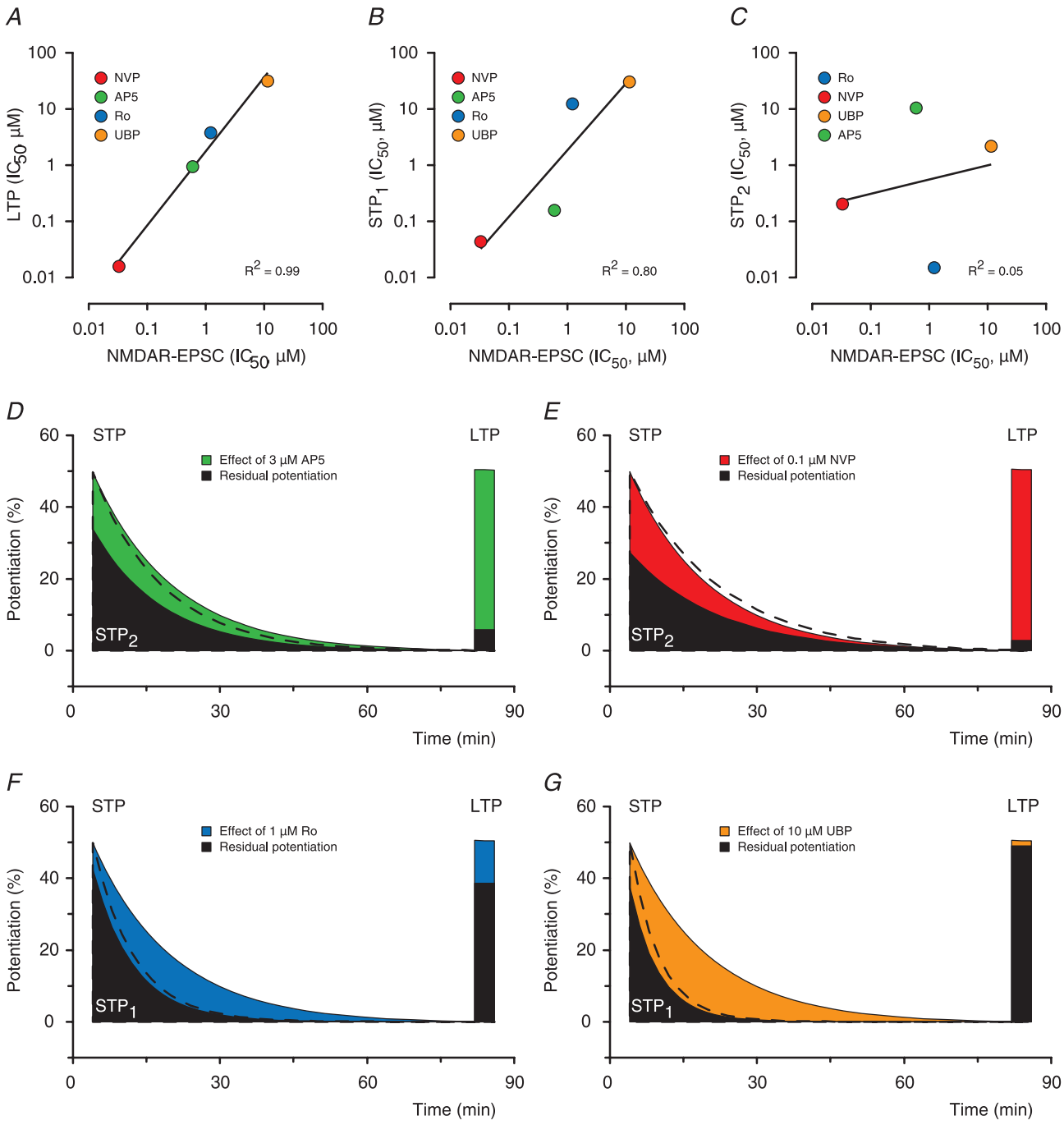

Figure 8. Three components of synaptic potentiation
A, IC_{50} values for the inhibition of NMDAR-EPSCs by the four antagonists and the IC_{50} values for their inhibition of LTP are strongly correlated ($P < 0.01$, NVP > AP5 > Ro > UBP). *B*, Inhibition of STP_1 is more weakly correlated with inhibition of NMDAR-EPSC but shows the same rank order of potency as LTP ($P = 0.1$, NVP > AP5 > Ro > UBP). *C*, Inhibition of STP_2 is not correlated with inhibition of NMDAR-EPSC and shows a different rank order of potency than STP_1 or LTP ($P = 0.8$, Ro > NVP > UBP > AP5). *D*, AP5 (3 μM) substantially inhibits LTP and reduces the amplitude of STP with little effect on its decay time constant. Effects on the decay of STP are visualized by scaling the amplitude (black dashed line) of the residual component (filled area) to that of the control (green area). *E*, 0.1 μM NVP has similar effects as 3 μM AP5. *F*, 1 μM Ro mainly affects the decay of STP. *G*, 10 μM UBP has similar effects as 1 μM Ro.

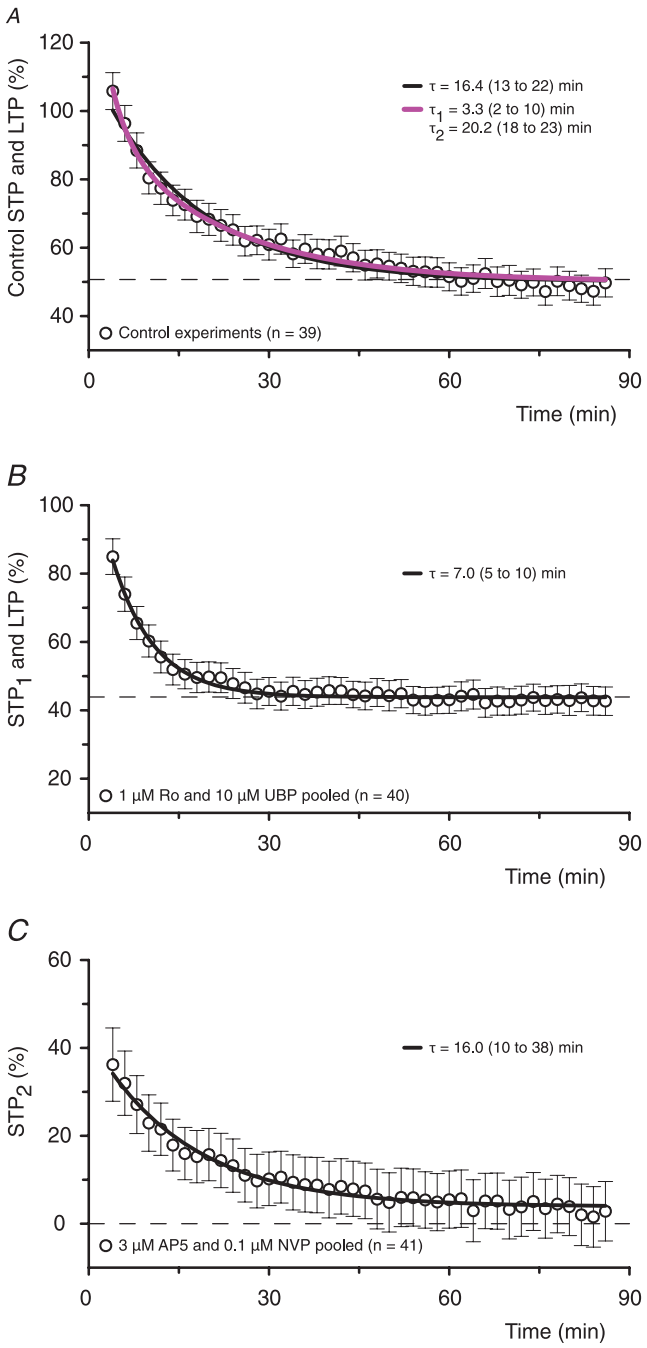

Figure 9. Two components of STP coexist at synapses with LTP
A, in the control experiments the declining phase of potentiation is fitted better by a double exponential model (purple line) than a single exponential model (black line, $P < 0.0001$, F test). Values of τ are shown for both models and their 95% confidence intervals (CI) are reported in parentheses. The residual potentiation is LTP. *B*, in experiments with 1 μM Ro or 10 μM UBP (to block STP_2), STP_1 declines in a mono-exponential fashion ($P = 0.7$, when compared to a double exponential model) to a stable level of sustained LTP (LTP: 43.9%; CI: 42.3–45.4%). *C*, In experiments with 3 μM AP5 or 0.1 μM NVP (to block STP_1), STP_2 declines mono-exponentially ($P = 0.8$, when compared to a double exponential model) to an LTP level of 3.9% (CI: 0.26–7.6%). Note that in terms of the area, STP_2 accounts for approximately 75% of the total STP.

also Feng *et al.* 2004). As expected, Ro was highly selective at GluN2B-containing receptors (Fischer *et al.* 1997), showing no inhibition of GluN2D-containing receptors. We did, however, confirm that Ro inhibits GluN2A-containing receptors at very high concentrations (Fischer *et al.* 1997). Furthermore, the maximal inhibition of GluN2B but not GluN2A-containing receptors by Ro was agonist concentration-dependent with greater inhibition found at higher agonist concentrations (Fischer *et al.* 1997). Given this, and other complexities in the non-competitve action of Ro, caution is needed when interpreting the results of this compound (Fischer *et al.* 1997; Hatton & Paoletti, 2005; Paoletti & Neyton, 2007). We also characterized in detail UBP145 (Costa *et al.* 2009) and found that it inhibits GluN2D-containing receptors more potently than GluN2A- or GluN2B-containing receptors, which were inhibited equally by this compound. Clearly, with the exception of Ro, these antagonists are not sufficiently selective for firm conclusions to be drawn when used in isolation. However, by comparing their relative potencies it is possible to make firm conclusions about the roles of NMDAR subtypes in the induction of STP and LTP. For this reason we have constructed full concentration–response curves for each of the antagonists and have based our conclusions on comparative criteria.

Role of NMDAR subtypes in LTP

There is evidence from knockout mice for a role of both GluN2A- and GluN2B-containing NMDARs in LTP (Sakimura *et al.* 1995; Kiyama *et al.* 1998; Weitlauf *et al.* 2005; von Engelhardt *et al.* 2008). The observation that LTP is highly sensitive to NVP is in agreement with previous observations using this antagonist (Liu *et al.* 2004; Berberich *et al.* 2005, 2007; Weitlauf *et al.* 2005; Bartlett *et al.* 2007; Li *et al.* 2007) and it has been suggested that GluN2A-containing receptors are important for induction of LTP (Liu *et al.* 2004). The possibility that this could be due to its inhibition of GluN2D-containing receptors is extremely unlikely, given that UBP only affected LTP at concentrations that inhibited GluN2A- and GluN2B-containing receptors. A similar conclusion was reached previously based on the relative insensitivity of LTP to a different, less selective, GluN2D antagonist (+/−)-cis-1-(phenanthren-2yl-carbonyl)-piperazine-2,3-dicarboxylic acid (Hrabetova *et al.* 2000). Pharmacological evidence for an involvement of GluN2B subunit-containing NMDARs in the induction of LTP is also well documented (Hrabetova *et al.* 2000; Bartlett *et al.* 2007; Berberich *et al.* 2007; Li *et al.* 2007). Thus, based on these various studies, it can be concluded that both GluN2A and GluN2B subunits are involved in the induction of LTP at CA3–CA1 synapses.

In our study, LTP was inhibited by Ro with an IC_{50} of 3 μM, which is in agreement with our earlier study that

used a high concentration of Ro (5 μM) at the CA3–CA1 synapses of juvenile rats (Bartlett *et al.* 2007), whereas studies that used lower concentrations of this or related compounds have reported less or no inhibition of LTP (Liu *et al.* 2004; Berberich *et al.* 2007; Li *et al.* 2007; Papouin *et al.* 2012). Therefore, the results can be best explained by the sensitivity of LTP to concentration-dependent inhibition by this class of GluN2B antagonist.

Notably, Ro had no effect on LTP at the concentration range over which it inhibits GluN1/GluN2B diheteromers, suggesting that these species are not involved it its induction. We can discount the possibility that sub-micromolar concentrations of Ro are unable to antagonize GluN2B-containing receptors in a physiological context, as STP was sensitive to Ro at these concentrations. Although we found that Ro can inhibit GluN2A subunits, this occurred at much higher concentrations than those that blocked LTP ($IC_{50} > 60\ \mu$M, see also Fischer *et al.* 1997). The most likely explanation of our findings is therefore that Ro inhibits LTP via antagonism of GluN1/GluN2A/GluN2B triheteromers, which have been shown to have an intermediate sensitivity to this class of inhibitor (Hatton & Paoletti, 2005; Gray *et al.* 2011) and are expressed at CA1 synapses of adult rodents (Rauner & Kohr, 2011).

Interestingly, there was a very strong correlation between the ability of all four compounds to antagonize the NMDAR-EPSC and LTP. This is entirely consistent with the widely held view that the NMDARs that mediate the EPSC are also responsible for the induction of LTP. Thus, our results are most readily explained by LTP being induced via post-synaptic NMDARs, which comprise a mixture of GluN1/GluN2A diheteromers and GluN1/GluN2A/GluN2B triheteromers.

Role of NMDAR subtypes in STP

A surprising observation in this study was that STP could be separated pharmacologically into two distinct components. One component, which we refer to as STP_1, was antagonized with the same rank order potency as LTP (NVP > AP5 > Ro > UBP). The simplest explanation is that STP_1 represents an initial decremental phase of LTP, although we cannot exclude that it is an entirely distinct component of synaptic plasticity, which involves a similar class of NMDAR as LTP for its induction. The second component of STP, STP_2, has a completely different sensitivity to NMDAR antagonists with a rank order potency of Ro > NVP > UBP > AP5. STP_1 and STP_2 also differ in their kinetics, such that STP_1 contributes largely to the peak of STP whereas STP_2 dominates its decay.

The sensitivity of STP_2 to all four antagonists is consistent with the involvement of both GluN2B- and GluN2D- but not GluN2A-containing NMDARs. The high sensitivity of STP_2 to Ro, compared to STP_1, LTP and NMDAR-EPSCs, suggests that the GluN2B subunit that is involved in its induction is not part of a triheteromeric NMDAR comprising GluN1/GluN2A/GluN2B subunits. The low sensitivity to AP5 also argues against a role of the GluN2A subunit in STP_2 but is consistent with a role of the GluN2D subunit (Ikeda *et al.* 1992; Buller & Monaghan, 1997). In support of this, the high sensitivity of STP_2 to both UBP and NVP is fully consistent with a role of GluN2D subunits. The observation that maximally effective concentrations of UBP and Ro are not additive could be explained by either the existence of two distinct GluN2B- and GluN2D-containing subtypes, which both need to be activated for STP_2 to be induced, or, more simply, by a single population of GluN1/GluN2B/GluN2D triheteromers. Interestingly, triheteromers of this composition have been described in the CNS (Pina-Crespo & Gibb, 2002; Brickley *et al.* 2003; Jones & Gibb, 2005; Brothwell *et al.* 2008). GluN2B/2D-containing receptors that are responsible for the induction of STP_2 at the CA3–CA1 synapses might be expressed either extra- (Lozovaya *et al.* 2004) or pre-synaptically (Thompson *et al.* 2002; McGuinness *et al.* 2010), which would explain a lack of correlation between the inhibition of STP_2 and the inhibition of the NMDAR-EPSC.

In addition to identifying the NMDAR subtypes involved in STP, the pharmacological experiments showed that the two components of STP could exist independently of each other. Thus, blockade of STP_2 enabled STP_1 to be recorded together with LTP, whereas blockade of STP_1 and LTP enabled STP_2 to be recorded in isolation. It has been shown previously that STP, when it is co-induced with LTP, can be 'stored' in the absence of stimulation (Volianskis & Jensen, 2003). In this study we extended this observation and show that both STP_1 and STP_2 can be stored in the absence of stimulation. Both STP_1 and STP_2 decay in an activity-dependent manner that depends on the number, but not the frequency, of stimuli. However, their decay kinetics differ with estimated tau values of 7 and 16 min, respectively, with a test stimulation frequency of 0.067 Hz. In other words, STP_1 and STP_2 require approximately 28 and 64 stimuli, respectively, to decay to $1/e$ of their initial amplitude.

Functional significance of STP and LTP

Although the full physiological significance of STP and LTP remains to be determined, it is interesting to note that STP can be induced independently of LTP both *in vitro* (Kauer *et al.* 1988; Anwyl *et al.* 1989; Malenka, 1991; Colino *et al.* 1992; Kullmann *et al.* 1992; Erickson *et al.* 2010) and *in vivo* (Buschler *et al.* 2012). It has also been shown that STP and LTP can be either co-expressed

or expressed independently of each other at the level of single synapses (Debanne *et al.* 1999). Thus, STP can be thought of as an independent process, and a phenomenon that resembles STP has been observed after exploratory learning in rats (Moser *et al.* 1993, Moser 1994).

There is a huge body of literature that equates NMDAR-LTP with learning and memory (Martin *et al.* 2000). However, this has usually assumed that NMDAR-LTP is a single process. Speculatively, if LTP indeed relates to long-term memory then STP could be used to store short-term memories. Short-term memory, or working memory, is actually a far more common occurrence with thousands of pieces of information stored for short periods of time but very few for long periods of time in any given day (Albright *et al.* 2000). If this is the case, then the prediction is that short-term working memory should be particularly sensitive to inhibition by GluN2B and GluN2D preferring antagonists.

The use-dependence of the decay of STP endows it with a particularly interesting functional property (Volianskis & Jensen, 2003). It could, in principle, store information up until the point of recall, assuming that recall involves reactivation of the same synapses that are used to encode the memory (Albright *et al.* 2000). This would be particularly useful for storing information for variable periods of time until the information is, once recalled, no longer of relevance: for example, remembering where one last placed one's cell phone.

The findings of the present study add to the current knowledge about STP and LTP by showing that NMDAR-dependent potentiation at the CA3–CA1 synapses in the hippocampus is more complex process than generally thought. In terms of induction, we have identified three components of synaptic potentiation that involve the activation of different NMDAR subtypes. A major component of STP involves receptors containing GluN2B and GluN2D subunits whereas LTP involves receptors containing GluN2A and GluN2B subunits.

References

Albright TD, Jessell TM, Kandel ER & Posner MI (2000). Neural science: a century of progress and the mysteries that remain. *Neuron* **25** (Suppl.), S1–55.

Andersen P, Sundberg SH, Sveen O & Wigstrom H (1977). Specific long-lasting potentiation of synaptic transmission in hippocampal slices. *Nature* **266**, 736–737.

Anegawa NJ, Lynch DR, Verdoorn TA & Pritchett DB (1995). Transfection of *N*-methyl-D-aspartate receptors in a nonneuronal cell line leads to cell death. *J Neurochem* **64**, 2004–2012.

Anwyl R, Mulkeen D & Rowan MJ (1989). The role of *N*-methyl-D-aspartate receptors in the generation of short-term potentiation in the rat hippocampus. *Brain Res* **503**, 148–151.

Auberson YP, Allgeier H, Bischoff S, Lingenhoehl K, Moretti R & Schmutz M (2002). 5-Phosphonomethylquinoxalinediones as competitive NMDA receptor antagonists with a preference for the human 1A/2A, rather than 1A/2B receptor composition. *Bioorg Med Chem Lett* **12**, 1099–1102.

Bartlett TE, Bannister NJ, Collett VJ, Dargan SL, Massey PV, Bortolotto ZA, Fitzjohn SM, Bashir ZI, Collingridge GL & Lodge D (2007). Differential roles of NR2A and NR2B-containing NMDA receptors in LTP and LTD in the CA1 region of two-week old rat hippocampus. *Neuropharmacology* **52**, 60–70.

Berberich S, Jensen V, Hvalby O, Seeburg PH & Kohr G (2007). The role of NMDAR subtypes and charge transfer during hippocampal LTP induction. *Neuropharmacology* **52**, 77–86.

Berberich S, Punnakkal P, Jensen V, Pawlak V, Seeburg PH, Hvalby O & Kohr G (2005). Lack of NMDA receptor subtype selectivity for hippocampal long-term potentiation. *J Neurosci* **25**, 6907–6910.

Bliss TV & Collingridge GL (1993). A synaptic model of memory: long-term potentiation in the hippocampus. *Nature* **361**, 31–39.

Bliss TV & Lomo T (1973). Long-lasting potentiation of synaptic transmission in the dentate area of the anaesthetized rabbit following stimulation of the perforant path. *J Physiol* **232**, 331–356.

Brickley SG, Misra C, Mok MH, Mishina M & Cull-Candy SG (2003). NR2B and NR2D subunits coassemble in cerebellar Golgi cells to form a distinct NMDA receptor subtype restricted to extrasynaptic sites. *J Neurosci* **23**, 4958–4966.

Brothwell SL, Barber JL, Monaghan DT, Jane DE, Gibb AJ & Jones S (2008). NR2B- and NR2D-containing synaptic NMDA receptors in developing rat substantia nigra pars compacta dopaminergic neurones. *J Physiol* **586**, 739–750.

Buller AL, Larson HC, Schneider BE, Beaton JA, Morrisett RA & Monaghan DT (1994). The molecular basis of NMDA receptor subtypes: native receptor diversity is predicted by subunit composition. *J Neurosci* **14**, 5471–5484.

Buller AL & Monaghan DT (1997). Pharmacological heterogeneity of NMDA receptors: characterization of NR1a/NR2D heteromers expressed in *Xenopus* oocytes. *Eur J Pharmacol* **320**, 87–94.

Buschler A, Goh JJ & Manahan-Vaughan D (2012). Frequency dependency of NMDA receptor-dependent synaptic plasticity in the hippocampal CA1 region of freely behaving mice. *Hippocampus* **22**, 2238–2248.

Chazot PL, Coleman SK, Cik M & Stephenson FA (1994). Molecular characterization of *N*-methyl-D-aspartate receptors expressed in mammalian cells yields evidence for the coexistence of three subunit types within a discrete receptor molecule. *J Biol Chem* **269**, 24403–24409.

Christie JM, Jane DE & Monaghan DT (2000). Native *N*-methyl-D-aspartate receptors containing NR2A and NR2B subunits have pharmacologically distinct competitive antagonist binding sites. *J Pharmacol Exp Ther* **292**, 1169–1174.

Colino A, Huang YY & Malenka RC (1992). Characterization of the integration time for the stabilization of long-term potentiation in area CA1 of the hippocampus. *J Neurosci* **12**, 180–187.

Collett VJ & Collingridge GL (2004). Interactions between NMDA receptors and mGlu5 receptors expressed in HEK293 cells. *Br J Pharmacol* **142**, 991–1001.

Collingridge GL, Kehl SJ & McLennan H (1983). Excitatory amino acids in synaptic transmission in the Schaffer collateral–commissural pathway of the rat hippocampus. *J Physiol* **334**, 33–46.

Collingridge GL, Olsen RW, Peters J & Spedding M (2009). A nomenclature for ligand-gated ion channels. *Neuropharmacology* **56**, 2–5.

Costa BM, Feng B, Tsintsadze TS, Morley RM, Irvine MW, Tsintsadze VP, Lozovaya NA, Jane DE & Monaghan DT (2009). NMDA receptor NR2 subunit selectivity of a series of novel piperazine-2,3-dicarboxylate derivatives; preferential blockade of extrasynaptic NMDA receptors in the rat hippocampal CA3–CA1 synapse. *J Pharmacol Exp Ther* **331**, 618–626.

Davies J, Francis AA, Jones AW & Watkins JC (1981). 2-Amino-5-phosphonovalerate (2APV), a potent and selective antagonist of amino acid-induced and synaptic excitation. *Neurosci Lett* **21**, 77–81.

Debanne D, Gahwiler BH & Thompson SM (1999). Heterogeneity of synaptic plasticity at unitary CA3–CA1 and CA3–CA3 connections in rat hippocampal slice cultures. *J Neurosci* **19**, 10664–10671.

Erickson MA, Maramara LA & Lisman J (2010). A single brief burst induces GluR1-dependent associative short-term potentiation: a potential mechanism for short-term memory. *J Cogn Neurosci* **22**, 2530–2540.

Feng B, Tse HW, Skifter DA, Morley R, Jane DE & Monaghan DT (2004). Structure–activity analysis of a novel NR2C/NR2D-preferring NMDA receptor antagonist: 1-(phenanthrene-2-carbonyl) piperazine-2,3-dicarboxylic acid. *Br J Pharmacol* **141**, 508–516.

Fischer G, Mutel V, Trube G, Malherbe P, Kew JN, Mohacsi E, Heitz MP & Kemp JA (1997). Ro 25–6981, a highly potent and selective blocker of *N*-methyl-D-aspartate receptors containing the NR2B subunit. Characterization *in vitro*. *J Pharmacol Exp Ther* **283**, 1285–1292.

Gray JA, Shi Y, Usui H, During MJ, Sakimura K & Nicoll RA (2011). Distinct modes of AMPA receptor suppression at developing synapses by GluN2A and GluN2B: single-cell NMDA receptor subunit deletion *in vivo*. *Neuron* **71**, 1085–1101.

Gustafsson B & Wigstrom H (1990). Long-term potentiation in the hippocampal CA1 region: its induction and early temporal development. *Prog Brain Res* **83**, 223–232.

Hanse E & Gustafsson B (1994). Onset and stabilization of NMDA receptor-dependent hippocampal long-term potentiation. *Neurosci Res* **20**, 15–25.

Hatton CJ & Paoletti P (2005). Modulation of triheteromeric NMDA receptors by N-terminal domain ligands. *Neuron* **46**, 261–274.

Hrabetova S, Serrano P, Blace N, Tse HW, Skifter DA, Jane DE, Monaghan DT & Sacktor TC (2000). Distinct NMDA receptor subpopulations contribute to long-term potentiation and long-term depression induction. *J Neurosci* **20**, RC81.

Ikeda K, Nagasawa M, Mori H, Araki K, Sakimura K, Watanabe M, Inoue Y & Mishina M (1992). Cloning and expression of the $\varepsilon 4$ subunit of the NMDA receptor channel. *FEBS Lett* **313**, 34–38.

Jones S & Gibb AJ (2005). Functional NR2B- and NR2D-containing NMDA receptor channels in rat substantia nigra dopaminergic neurones. *J Physiol* **569**, 209–221.

Karakas E, Simorowski N & Furukawa H (2011). Subunit arrangement and phenylethanolamine binding in GluN1/GluN2B NMDA receptors. *Nature* **475**, 249–253.

Kauer JA, Malenka RC & Nicoll RA (1988). NMDA application potentiates synaptic transmission in the hippocampus. *Nature* **334**, 250–252.

Kiyama Y, Manabe T, Sakimura K, Kawakami F, Mori H & Mishina M (1998). Increased thresholds for long-term potentiation and contextual learning in mice lacking the NMDA-type glutamate receptor epsilon1 subunit. *J Neurosci* **18**, 6704–6712.

Kullmann DM, Perkel DJ, Manabe T & Nicoll RA (1992). Ca^{2+} entry via postsynaptic voltage-sensitive Ca^{2+} channels can transiently potentiate excitatory synaptic transmission in the hippocampus. *Neuron* **9**, 1175–1183.

Larson J & Lynch G (1988). Role of *N*-methyl-D-aspartate receptors in the induction of synaptic potentiation by burst stimulation patterned after the hippocampal theta-rhythm. *Brain Res* **441**, 111–118.

Larson J, Wong D & Lynch G (1986). Patterned stimulation at the theta frequency is optimal for the induction of hippocampal long-term potentiation. *Brain Res* **368**, 347–350.

Li R, Huang FS, Abbas AK & Wigstrom H (2007). Role of NMDA receptor subtypes in different forms of NMDA-dependent synaptic plasticity. *BMC Neurosci* **8**, 55.

Liu L, Wong TP, Pozza MF, Lingenhoehl K, Wang Y, Sheng M, Auberson YP & Wang YT (2004). Role of NMDA receptor subtypes in governing the direction of hippocampal synaptic plasticity. *Science* **304**, 1021–1024.

Lozovaya NA, Grebenyuk SE, Tsintsadze T, Feng B, Monaghan DT & Krishtal OA (2004). Extrasynaptic NR2B and NR2D subunits of NMDA receptors shape 'superslow' afterburst EPSC in rat hippocampus. *J Physiol* **558**, 451–463.

Malenka RC (1991). Postsynaptic factors control the duration of synaptic enhancement in area CA1 of the hippocampus. *Neuron* **6**, 53–60.

Martin SJ, Grimwood PD & Morris RG (2000). Synaptic plasticity and memory: an evaluation of the hypothesis. *Annu Rev Neurosci* **23**, 649–711.

Massey PV, Johnson BE, Moult PR, Auberson YP, Brown MW, Molnar E, Collingridge GL & Bashir ZI (2004). Differential roles of NR2A and NR2B-containing NMDA receptors in cortical long-term potentiation and long-term depression. *J Neurosci* **24**, 7821–7828.

McGuinness L, Taylor C, Taylor RD, Yau C, Langenhan T, Hart ML, Christian H, Tynan PW, Donnelly P & Emptage NJ (2010). Presynaptic NMDARs in the hippocampus facilitate transmitter release at theta frequency. *Neuron* **68**, 1109–1127.

Monyer H, Burnashev N, Laurie DJ, Sakmann B & Seeburg PH (1994). Developmental and regional expression in the rat brain and functional properties of four NMDA receptors. *Neuron* **12**, 529–540.

Morley RM, Tse HW, Feng B, Miller JC, Monaghan DT & Jane DE (2005). Synthesis and pharmacology of N1-substituted piperazine-2,3-dicarboxylic acid derivatives acting as NMDA receptor antagonists. *J Med Chem* **48**, 2627–2637.

Moser E, Moser MB & Andersen P (1993). Synaptic potentiation in the rat dentate gyrus during exploratory learning. *Neuroreport* **5**, 317–320.

Moser EI, Moser MB & Andersen P (1994). Potentiation of dentate synapses initiated by exploratory learning in rats: dissociation from brain temperature, motor activity, and arousal. *Learn Mem* **1**, 55–73.

Pananceau M & Gustafsson B (1997). NMDA receptor dependence of the input specific NMDA receptor-independent LTP in the hippocampal CA1 region. *Brain Res* **752**, 255–260.

Paoletti P & Neyton J (2007). NMDA receptor subunits: function and pharmacology. *Curr Opin Pharmacol* **7**, 39–47.

Papouin T, Ladepeche L, Ruel J, Sacchi S, Labasque M, Hanini M, Groc L, Pollegioni L, Mothet JP & Oliet SH (2012). Synaptic and extrasynaptic NMDA receptors are gated by different endogenous coagonists. *Cell* **150**, 633–646.

Pina-Crespo JC & Gibb AJ (2002). Subtypes of NMDA receptors in new-born rat hippocampal granule cells. *J Physiol* **541**, 41–64.

Rauner C & Kohr G (2011). Triheteromeric NR1/NR2A/NR2B receptors constitute the major *N*-methyl-D-aspartate receptor population in adult hippocampal synapses. *J Biol Chem* **286**, 7558–7566.

Sakimura K, Kutsuwada T, Ito I, Manabe T, Takayama C, Kushiya E, Yagi T, Aizawa S, Inoue Y, Sugiyama H *et al.* (1995). Reduced hippocampal LTP and spatial learning in mice lacking NMDA receptor epsilon 1 subunit. *Nature* **373**, 151–155.

Schulz PE & Fitzgibbons JC (1997). Differing mechanisms of expression for short- and long-term potentiation. *J Neurophysiol* **78**, 321–334.

Thompson CL, Drewery DL, Atkins HD, Stephenson FA & Chazot PL (2002). Immunohistochemical localization of *N*-methyl-D-aspartate receptor subunits in the adult murine hippocampal formation: evidence for a unique role of the NR2D subunit. *Brain Res Mol Brain Res* **102**, 55–61.

Vicini S, Wang JF, Li JH, Zhu WJ, Wang YH, Luo JH, Wolfe BB & Grayson DR (1998). Functional and pharmacological differences between recombinant *N*-methyl-D-aspartate receptors. *J Neurophysiol* **79**, 555–566.

Volianskis A & Jensen MS (2003). Transient and sustained types of long-term potentiation in the CA1 area of the rat hippocampus. *J Physiol* **550**, 459–492.

Volianskis A, Kostner R, Molgaard M, Hass S & Jensen MS (2010). Episodic memory deficits are not related to altered glutamatergic synaptic transmission and plasticity in the CA1 hippocampus of the APPswe/PS1DE9-deleted transgenic mice model of β-amyloidosis. *Neurobiol Aging* **31**, 1173–1187.

von Engelhardt J, Doganci B, Jensen V, Hvalby O, Gongrich C, Taylor A, Barkus C, Sanderson DJ, Rawlins JN, Seeburg PH, Bannerman DM & Monyer H (2008). Contribution of hippocampal and extra-hippocampal NR2B-containing NMDA receptors to performance on spatial learning tasks. *Neuron* **60**, 846–860.

Weitlauf C, Honse Y, Auberson YP, Mishina M, Lovinger DM & Winder DG (2005). Activation of NR2A-containing NMDA receptors is not obligatory for NMDA receptor-dependent long-term potentiation. *J Neurosci* **25**, 8386–8390.

Author contributions

All experiments were performed at the University of Bristol, UK. A.V., N.B., M.S.J. and G.L.C. designed the study. A.V., N.B., V.J.C. and M.W.J. performed the experiments and analysed the data. D.T.M., D.E.J. and G.L.C. supervised chemical, pharmacological and physiological investigations. A.V., N.B. and S.F.M. wrote the first draft of the manuscript. All authors have read, commented on and approved the final version.

Acknowledgements

The study was supported by the Danish Medical Research Council (271-05-0712), the MRC (G0601812), the NIH (MH60252) and the Welcome Trust. The authors declare no competing financial interests.